Acta Mech 226, 1201–1212 (2015)
DOI 10.1007/s00707-014-1220-3

Fangwei Qiang · Peijun Wei

Effective dynamic properties of random nanoporous materials with consideration of surface effects

Received: 14 April 2014 / Revised: 10 July 2014 / Published online: 9 October 2014
© Springer-Verlag Wien 2014

Abstract The frequency-dependent dynamic effective properties (velocity, attenuation and elastic modulus) of nanoporous materials with randomly positioned spherical cavities are studied. The surface energy theory proposed by Huang and Wang (Handbook of micromechanics and nanomechanics. Pan Stanford Publishing Pte Ltd., Singapore, pp 303–348, 2013) is used to derive the non-traditional boundary condition on the surface of the nanocavity and further the scattering matrix of a single nanocavity. Then, the total wave field is obtained by considering the multiple scattering processes among the dispersive spherical cavities. The configuration average of the total wave field results in the coherent waves or the averaged waves. The numerical examples of the effective speed, the effective attenuation of the coherent waves and associated effective dynamic modulus of a nanoporous material are given and shown graphically. The effects of surface elasticity and the residual surface tension are both considered. Moreover, the influences of the non-symmetric parts of in-plane surface stress and the out-of-plane parts of the surface stress are also discussed based on the numerical examples.

1 Introduction

The propagation of elastic waves in a composite material with randomly distributed particles was an interesting subject in the past decades [1–5]. Waterman and Truell [1] studied the multiple scattering effects due to a random array of obstacles and gave the complex propagation constant of the scattering medium in the limit of vanishing correlations in position. The effective phase speed and the attenuation of the coherent compressional wave and shear wave in a particulate-reinforced composite medium were discussed by Datta et al. in [2], and the interface layer effects in the particulate-reinforced composite medium were considered in [3,4]. Further studies on the effect of a viscoelastic interlayer between the reinforced particle and the matrix material were presented by Wei and Huang in [5]. Their investigations showed that the attenuation of the effective waves is related to both the multiple scattering among reinforced particles and the material dissipation of the viscoelastic interphase. Because of the complicated nature of the multiple scattering problems, the effective field approximation and the effective medium are often used to simplify the problem in low filling rate composites. However, they may not be satisfying approximations for high filling rate composites. In order to describe the effective properties of high fill rate composites, Varadan et al. [6] studied the multiple scattering waves in a composite by introducing pair-correlation function to describe the interaction between two scatterers. Using a combination of the pair-correlation function and the effective field approach, Kanaun [7] calculated the effective properties of dielectric

F. Qiang · P. Wei
Department of Applied Mechanics, University of Science and Technology Beijing, Beijing 100083, China

P. Wei (✉)
State Key Laboratory of Nonlinear Mechanics (LNM), Chinese Academy of Science, Beijing 100080, China
E-mail: weipj@ustb.edu.cn
Tel: 86-10-82388981

matrix composite materials with high filling rate of inclusions. Recently, the pair-correlation function together with quasi-crystalline approximation was also used by Fang et al. [8] to investigate the multiple scattering of the P wave and S wave in composite materials with high volume concentrations of particles.

At the atomic scale, the local environment at and near a surface (or an interface) is quite different from that in the bulk material. This can be described macroscopically by the excess free energy of a surface (or an interface) and the corresponding surface/interface stresses. The effects of the surface (or the interface) stresses of embedded inclusions on the overall properties of the composites are not negligible anymore in the size range of tens of nanometers, where the surface/interface effects are enhanced by a significant surface-to-volume ratio. During the past half-century, increasing interest has been paid to study the surface/interface problems among materials scientists and engineers [9–17]. A linearized theory of surface elasticity proposed by Gurtin and Murdoch [10,11] (G–M model for brevity) has attracted considerable attention and been widely used to study the elastic behavior of solids at micro/nanoscales [12–15]. However, considerable inconsistence has occurred in the interpretation of the G–M model, and different versions have been used in the literature without clear identification of the underlying assumptions as reviewed by Ru [18]. In the wave motion problem, the diffraction of elastic waves with surface effects has been studied by Wang [19,20]. However, only the dynamic stress concentration factor of a single scatterer is considered and the multiple scattering waves from dispersive scatterers were not included in their works. Recently, the effective propagation constants of coherent waves in nanocomposite materials with dispersive cylindrical nanofibers and nanocavities were discussed by Qiang and Wei [21,22]. It was shown that the effects of the surface (or interface) stress is evident for nanoscale fibers or cavities and gradually diminishes when the size of fibers or cavities increases. Based on the effective medium approximation, Hasheminejad and Avazmohammadi [23] also studied the effective propagation constants of the elastic waves in a composite reinforced by parallel nanofibers. However, it should be pointed out that in all above-mentioned works on the wave motion in nanocomposites, the basic equations of the surface/interface were not properly utilized, as will be explained in the following. According to the surface/interface energy theory proposed by Huang and Wang [24,25], several key issues should be addressed: (1) It is important to note that the creation of a surface or interface will generally result in a surface stress (referred to as "residual surface tension"), thus there will exist a surface or interface-induced residual stress field in the bulk under no external loading. Therefore, even in infinitesimal deformation approximations, the first and second Piola–Kirchhoff surface stresses, and the Cauchy surface stress are not the same due to the existence of the residual surface tension. (2) Generally, the exact position (e.g., the shape and size, and hence the curvature tensor) of the deformed surface/interface is not known in advance. Therefore, in the study of the mechanical properties of nanocomposites, it is necessary to use the Lagrangian description of the surface equilibrium equation relative to the reference configuration. Furthermore, as the first Piola–Kirchhoff surface stress appears in this description, it is natural to express the surface constitutive relations in terms of the first Piola–Kirchhoff surface stress, and both in-plane term and out-of plane term of this surface stress should be included. (3) The effects of residual surface tension and surface elasticity on the effective properties of nanocomposites should be considered and both of them are shown to be important.

In this paper, a new equation of surface given by Huang and Wang [25] is employed. The effective propagation constants of coherent waves and the associated effective dynamic elastic modulus are estimated. Some numerical examples are given graphically and the comparison with those obtained from two simplified versions of the present model are presented. The effects of surface elasticity and the residual surface tension are both considered in the numerical results. The influences of the non-symmetric parts of in-plane surface stress and the out-of-plane parts of the surface stress are also discussed based on the numerical examples.

2 Governing equations at the surface and in the bulk material

Now consider a smooth surface A_0 of a nanocavity in a porous material undergoing neither body force, nor any external surface traction/displacement on its boundary, which corresponds to the reference configuration. However, in this reference configuration, there exists the residual stress field $\boldsymbol{\sigma}^*$ in the bulk material induced by the "residual surface tension". The covariant base vectors of the surface A_0 are $\mathbf{A}_\alpha(\alpha = 1, 2)$, with the unit normal vector to the surface A_0 denoted by $\mathbf{A}_3$. The contra-variant base vectors of the surface A_0 are $\mathbf{A}^\alpha(\alpha = 1, 2)$ satisfying the relation $\mathbf{A}_\alpha \cdot \mathbf{A}^\beta = \delta_\alpha^\beta \quad (\alpha, \beta = 1, 2)$, where δ_α^β is the Kronecker delta symbol in a 2-D space. It is noted both $\mathbf{A}_\alpha$ and $\mathbf{A}^\beta$ are in the tangent plane of the surface A_0. The displacement $\mathbf{u}$ on the surface can be expressed in terms of the base vectors $(\mathbf{A}_1, \mathbf{A}_2, \mathbf{A}_3)$ in the reference configuration:

$$\mathbf{u} = u_0^\beta \mathbf{A}_\beta + u_0^n \mathbf{A}_3 \quad (\text{summation over } \beta). \tag{1}$$

The deformation gradient of the surface is given by

$$\mathbf{F}_s = \mathbf{i}_0 + (\mathbf{u}\nabla_{0s})^{(\mathrm{in})} + (\mathbf{u}\nabla_{0s})^{(\mathrm{out})} = \mathbf{F}_s^{(\mathrm{in})} + \mathbf{F}_s^{(\mathrm{out})}, \tag{2}$$

where $\mathbf{i}_0$ is the second order identity tensor in the tangent plane of A_0, ∇_{0s} is the gradient operator of the surface at A_0 in the reference configuration. $\mathbf{F}_s^{(\mathrm{in})} = \mathbf{i}_0 + (\mathbf{u}\nabla_{0s})^{(\mathrm{in})}$ and $\mathbf{F}_s^{(out)} = (\mathbf{u}\nabla_{0s})^{(\mathrm{out})} = d_\beta \mathbf{A}_3 \otimes \mathbf{A}^\beta$ correspond to the in-plane term and the out-of-plane term of the surface deformation gradient, respectively. $(\mathbf{u}\nabla_{0s})^{(\mathrm{in})}$ is the in-plane part of the surface displacement gradient and is defined by

$$(\mathbf{u}_0\nabla_{0s})^{(\mathrm{in})} = \mathbf{u}_{0s}\nabla_{0s} - u_0^n\mathbf{b}_0 = u_0^\lambda|_\beta \mathbf{A}_\lambda \otimes \mathbf{A}^\beta - u_0^n\mathbf{b}_0, \tag{3}$$

where $\mathbf{u}_0 = \mathbf{u}_{0s} + \mathbf{u}_{0n}$ ($\mathbf{u}_{0s}$ and $\mathbf{u}_{0n}$ are the in-plane part and the out-of-plane part of displacement vector) and $d_\beta = u_0^\lambda b_{0\lambda\beta} + u_0^n|_\beta$. $\mathbf{b}_0 = b_{0\lambda\alpha}\mathbf{A}^\lambda \otimes \mathbf{A}^\alpha$ is the curvature tensor of the surface A_0.

There are two fundamental equations of the surface. The first one is the constitutive relation of the surface and the second one is the equation of motion (equilibrium) of the surface. In the following, only the infinitesimal deformation is considered and the surface is assumed to be isotropic. In the Lagrangian description, the constitutive relation of the surface expressed in terms of the first Piola–Kirchhoff surface stress can be written as

$$\mathbf{S}_s = \sigma^0\mathbf{i}_0 + \Delta\mathbf{S}_s^{(\mathrm{in})} + \Delta\mathbf{S}_s^{(\mathrm{out})}, \tag{4}$$

where

$$\Delta\mathbf{S}_s^{(\mathrm{in})} = \left(\sigma^0 + \lambda^s\right)(\mathrm{tr}\mathbf{E}_s)\,\mathbf{i}_0 + 2\left(\mu^s - \sigma^0\right)\mathbf{E}_s + \sigma^0(\mathbf{u}\nabla_{0s})^{(\mathrm{in})}, \tag{5}$$

$$\Delta\mathbf{S}_s^{(\mathrm{out})} = \sigma^0\mathbf{F}_s^{(\mathrm{out})} = \sigma^0(\mathbf{u}\nabla_{0s})^{(\mathrm{out})}. \tag{6}$$

In the above equation, $\sigma^0\mathbf{i}_0$ is the residual surface stress, λ^s and μ^s are láme constants of the surface. $\mathbf{E}_s = \frac{1}{2}[(\mathbf{u}\nabla_{0s})^{(\mathrm{in})} + (\nabla_{0s}\mathbf{u})^{(\mathrm{in})}]$ is the surface strain.

The second fundamental equation of the surface is the equation of motion (equilibrium) of the surface. For a surface with zero thickness, the inertia force of the surface can be neglected. Hence only the equilibrium equation of the surface, i.e., the Young–Laplace equation needs to be considered. The Lagrangian descriptions of the Young–Laplace equation relative to the reference configuration can be written as

$$\mathbf{A}_3 \cdot [\![\Delta\mathbf{S}^0]\!] \cdot \mathbf{A}_3 = -\left(\Delta\mathbf{S}_s^{(\mathrm{in})}\right) : \mathbf{b}_0 - \left[\mathbf{A}_3 \cdot \left(\Delta\mathbf{S}_s^{(\mathrm{out})}\right)\right] \cdot \nabla_{0s}, \tag{7a}$$

$$\mathbf{P}_0 \cdot [\![\Delta\mathbf{S}^0]\!] \cdot \mathbf{A}_3 = -\left(\Delta\mathbf{S}_s^{(\mathrm{in})}\right) \cdot \nabla_{0s} - \left[\mathbf{A}_3 \cdot \left(\Delta\mathbf{S}_s^{(\mathrm{out})}\right) \cdot \mathbf{b}_0\right], \tag{7b}$$

where $\Delta\mathbf{S}^0 = \mathbf{S}^0 - \boldsymbol{\sigma}^*$, $\mathbf{S}^0$ and $\boldsymbol{\sigma}^*$ are the first Piola–Kirchhoff stress and the residual stress in the bulk material respectively, $\mathbf{P}_0 = \mathbf{I} - \mathbf{A}_3 \otimes \mathbf{A}_3$ is the projection operator on the tangent plane of the surface. $\mathbf{I}$ is the second-rank identity tensor in 3-dimensional space. $[\![\Delta\mathbf{S}^0]\!]$ is the discontinuity of $\Delta\mathbf{S}^0$ across the surface.

Next, consider the governing equations in the matrix material. A linearized constitutive relation with residual stress has been given by Hoger [26] and was discussed by Huang et al. [24,25]. The infinitesimal strain in the matrix material relative to the reference configuration is defined by

$$\boldsymbol{\varepsilon} = \frac{1}{2}(\mathbf{u}\nabla_0 + \nabla_0\mathbf{u}), \tag{8}$$

where $\mathbf{u}$ is the displacement from the reference configuration to the current configuration, ∇_0 denotes the gradient operator in 3-D space. The linearized elastic constitutive relation with the residual stress in the bulk material expressed in terms of the first Piola–Kirchhoff stress can be written as

$$\mathbf{S}^0 = \boldsymbol{\sigma}^* + (\mathbf{u}\nabla_0) \cdot \boldsymbol{\sigma}^* + \mathbf{L} : \boldsymbol{\varepsilon}, \tag{9}$$

where $\mathbf{L}$ is the elastic stiffness tensor. In the case that $\boldsymbol{\sigma}^*$ has the same order in magnitude as $\mathbf{L} : \boldsymbol{\varepsilon}$, the term $(\mathbf{u}\nabla_0) \cdot \boldsymbol{\sigma}^*$ in the above equation can be neglected. Therefore, for an isotopic elastic material, we have

$$\Delta\mathbf{S}^0 = \mathbf{S}^0 - \boldsymbol{\sigma}^* = \mathbf{L} : \boldsymbol{\varepsilon} = \lambda(\mathrm{tr}\boldsymbol{\varepsilon})\mathbf{I} + 2\mu\boldsymbol{\varepsilon}, \tag{10}$$

where λ and μ are the láme constants in the matrix material. The equation of motion in the bulk material is given by

$$\mathbf{S}^0 \cdot \nabla_0 + \rho_0\mathbf{f} = \rho_0\ddot{\mathbf{u}}, \tag{11}$$

where $\mathbf{f}$ is the body force and ρ_0 is the mass density. It is noted that the residual stress $\boldsymbol{\sigma}^*$ satisfies the equilibrium equation $\boldsymbol{\sigma}^* \cdot \nabla_0 = \mathbf{0}$, hence in the absence of body force, we have

$$\Delta \mathbf{S}^0 \cdot \nabla_0 = \rho_0 \ddot{\mathbf{u}}. \tag{12}$$

It is seen that the surface stress includes two parts, one is the in-plane parts and the other is the out-of-plane part, and both parts are non-symmetrical. These are consistent with the surface stress model proposed by Gurtin and Murdoch (G–M model). In both models (H–W model and G–M model), the deformation of bulk solid and the surface under external loading are thought to be a finite-deformation problem due to the existence of surface tension, even for an infinitesimal deformation. However, in a sense of Cauchy elasticity, Gurtin and Murdoch [10] presented a surface stress as the function of the deformation gradient. Huang and Wang [24,25] derived the surface constitutive relations for the hyperelastic media at finite deformation, where, in the Green elasticity, the surface stress is expressed in terms of the surface free energy. It is emphasized by Huang and Wang that the surface constitutive relation should be established based on the reference configuration without the external loading but with the residual stress field in the bulk caused by the surface tension. Equations (5) and (6) are the results of the infinitesimal deformation approximation and are same with the surface stress in the G–M model, i.e., Eq. (2) in [11]. It should be pointed out that there are two simplified versions which are specially interesting. One ignores the out-of-plane surface stress, i.e., $\Delta \mathbf{S}_s^{(\text{out})}$ (SM-I for brevity); The other further ignores the non-symmetric term of in-plane surface stress, i.e., $\sigma^0(\mathbf{u}\nabla_{0s})^{(\text{in})}$ (SM-II for brevity).

3 The individual scattering of a nanocavity

Let's consider a spherical cavity of radius a embedded in an infinite isotropic material. The time harmonic longitudinal wave with circular frequency ω is assumed to propagate along z-axis through the matrix material, which can be expressed by a displacement potential

$$\phi^i = \phi_0 e^{i(k_p z - \omega t)}, \tag{13}$$

where ϕ_0 is the amplitude of incident P wave. k_p is the wavenumber of P wave. When the incident wave impinges the spherical cavity, the scattered P wave and S wave are induced outside the cavity. The symmetry of spherical cavity results in $u_\varphi = 0$ and the independence of displacement u_r and u_θ on the spherical coordinate φ. Thus, the incident wave and the scattered wave can be expressed as

$$\phi^i = \phi_0 \sum_{n=0}^{\infty} (2n+1) i^n j_n(k_p r) P_n(\cos\theta) e^{-i\omega t}, \tag{14a}$$

$$\phi^r = \phi_0 \sum_{n=0}^{\infty} (2n+1) i^n A_n h_n^{(1)}(k_p r) P_n(\cos\theta) e^{-i\omega t}, \tag{14b}$$

$$\chi^r = \phi_0 \sum_{n=0}^{\infty} (2n+1) i^n B_n h_n^{(1)}(k_s r) P_n(\cos\theta) e^{-i\omega t}, \tag{14c}$$

where ϕ and χ are the dilatational and distortional displacement potentials. k_s is the wavenumber of S wave. $j_n(x)$, $h_n^{(1)}(x)$ and $P_n(x)$ are the nth order spherical Bessel function, spherical Hankel function and Legendre function, respectively. A_n and B_n are the unknown coefficients to be determined by the Young–Laplace equation and the surface constitutive relation of the nanosized spherical cavity in the present problem.

In the spherical polar coordinate system,

$$\mathbf{A}_3 = \mathbf{e}_r, \ \mathbf{b} = -[(1/r)\mathbf{e}_\theta \mathbf{e}_\theta + 0 \cdot \mathbf{e}_\theta \mathbf{e}_\varphi + 0 \cdot \mathbf{e}_\varphi \mathbf{e}_\theta + (1/r)\mathbf{e}_\varphi \mathbf{e}_\varphi], \tag{15}$$

$$\begin{aligned} (\mathbf{u} \ \nabla_{0s}) &= (u_r^s \mathbf{e}_r + u_\theta^s \mathbf{e}_\theta + u_\varphi^s \mathbf{e}_\varphi) \cdot \left(\frac{\partial}{r \partial \theta} \mathbf{e}_\theta + \frac{\partial}{r \sin\theta \partial \varphi} \mathbf{e}_\varphi \right) \\ &= (\mathbf{u}\nabla_{0s})^{(\text{in})} + (\mathbf{u}\nabla_{0s})^{(\text{out})}, \end{aligned} \tag{16}$$

$$\begin{aligned} (\mathbf{u}\nabla_{0s})^{(\text{in})} &= \mathbf{u}_s \nabla_{0s} - u_r \mathbf{b}_0 \\ &= \left(\frac{\partial u_\theta}{r \partial \theta} + \frac{u_r}{r} \right) \mathbf{e}_\theta \mathbf{e}_\theta + \left(\frac{\partial u_\theta}{r \sin\theta \partial \varphi} - \frac{u_\varphi}{r} \cot\theta \right) \mathbf{e}_\theta \mathbf{e}_\varphi \end{aligned}$$

$$+\frac{\partial u_\theta}{r\partial\theta}\mathbf{e}_\varphi\mathbf{e}_\theta+\left(\frac{\partial u_\theta}{r\sin\theta\partial\varphi}+\frac{u_\theta}{r}\cot\theta+\frac{u_r}{r}\right)\mathbf{e}_\varphi\mathbf{e}_\varphi, \tag{17}$$

$$\mathbf{E}^s=0.5\left[(\mathbf{u}\nabla_{0s})^{(\text{in})}+\left((\nabla_{0s}\mathbf{u})^{(\text{in})}\right)^T\right], \tag{18}$$

$$\mathbf{F}^{(\text{out})}=(\mathbf{u}\nabla_{0s})^{(\text{out})}=\left(\frac{\partial u_r}{r\partial\theta}-\frac{u_\theta}{r}\right)\mathbf{e}_r\mathbf{e}_\theta+\left(\frac{1}{r\sin\theta}\frac{\partial u_r}{\partial\varphi}-\frac{u_\varphi}{r}\right)\mathbf{e}_r\mathbf{e}_\varphi. \tag{19}$$

Let $\Delta\mathbf{S}_s^{(\text{in})}=\sigma^s_{\alpha\beta}\mathbf{e}_\alpha\mathbf{e}_\beta$, $\Delta\mathbf{S}_s^{(\text{out})}=\sigma^s_{r\beta}\mathbf{e}_r\mathbf{e}_\beta$, $(\alpha,\beta=\theta,\varphi)$, then, the explicit expressions of Eq. (7) are

$$t_r^b=-\left(\frac{\partial\sigma^s_{r\theta}}{r\partial\theta}+\frac{\partial\sigma^s_{r\varphi}}{r\sin\theta\partial\varphi}+\frac{\sigma^s_{r\theta}}{r}\cot\theta-\frac{\sigma^s_{\theta\theta}+\sigma^s_{\varphi\varphi}}{r}\right), \tag{20a}$$

$$t_\theta^b=-\left(\frac{\partial\sigma^s_{\theta\theta}}{r\partial\theta}+\frac{\partial\sigma^s_{\theta\varphi}}{r\sin\theta\partial\varphi}+\frac{\sigma^s_{\theta\theta}-\sigma^s_{\varphi\varphi}}{r}\cot\theta+\frac{\sigma^s_{r\theta}}{r}\right), \tag{20b}$$

$$t_\varphi^b=-\left(\frac{\partial\sigma^s_{\varphi\theta}}{r\partial\theta}+\frac{\partial\sigma^s_{\varphi\varphi}}{r\sin\theta\partial\varphi}+\frac{\sigma^s_{\theta\varphi}+\sigma^s_{\varphi\theta}}{r}\cot\theta+\frac{\sigma^s_{r\varphi}}{r}\right), \tag{20c}$$

where t_r^b and (t_θ^b,t_φ^b) are the normal and the tangential components of tractions $t_i^b\left(=\sigma_{ij}^b n_j\right)$ of the bulk material near the surface, respectively. Consider $u_\varphi=0$ and (u_r,u_θ) are independent of the spherical coordinate φ in the case of incident P wave. The surface stress can be expressed as

$$\sigma^s_{\theta\theta}=\left(\lambda^s+2\mu^s\right)\frac{\partial u_\theta}{r\partial\theta}+\left(\lambda^s+\sigma^0\right)\frac{u_\theta}{r}\cot\theta+\left(2\lambda^s+2\mu^s+\sigma^0\right)\frac{u_r}{r}, \tag{21a}$$

$$\sigma^s_{\varphi\varphi}=\left(\lambda^s+\sigma^0\right)\frac{\partial u_\theta}{r\partial\theta}+\left(\lambda^s+2\mu^s\right)\frac{u_\theta}{r}\cot\theta+\left(2\lambda^s+2\mu^s+\sigma^0\right)\frac{u_r}{r}, \tag{21b}$$

$$\sigma^s_{r\theta}=\sigma^0\left(\frac{\partial u_r}{r\partial\theta}-\frac{u_\theta}{r}\right),\ \sigma^s_{r\varphi}=0,\ \sigma^s_{\theta\varphi}=\sigma^s_{\varphi\theta}=0. \tag{21c}$$

Then, the surface equilibrium conditions can be further expressed in the displacement form

$$\begin{aligned}\sigma^b_{rr}\Big|_{r=a}=&\frac{1}{a^2}\left(\sigma^0+2\lambda^s+2\mu^s\right)\left(2u_r+u_\theta\cot\theta+\frac{\partial u_\theta}{\partial\theta}\right)\Big|_{r=a}\\&-\frac{\sigma^0}{a^2}\left(\frac{\partial^2u_r}{\partial\theta^2}-\frac{\partial u_\theta}{\partial\theta}+\frac{\partial u_r}{\partial\theta}\cot\theta-u_\theta\cot\theta\right)\Big|_{r=a},\end{aligned} \tag{22a}$$

$$\begin{aligned}\sigma^b_{r\theta}\Big|_{r=a}=&\frac{1}{a^2}\left[\left(2\sigma^0+\lambda^s\right)u_\theta+\left(\lambda^s+2\mu^s\right)\left(u_\theta\cot^2\theta-\frac{\partial u_\theta}{\partial\theta}\cot\theta-\frac{\partial^2u_\theta}{\partial\theta^2}\right)\right]\Big|_{r=a}\\&-\frac{2}{a^2}\left[\left(\sigma^0+\lambda^s+\mu^s\right)\frac{\partial u_r}{\partial\theta}\right]\Big|_{r=a}.\end{aligned} \tag{22b}$$

For the simplified models of surface stress, the surface equilibrium conditions reduces to

$$\sigma_{rr}|_{r=a}=\frac{\left(\sigma^0+2\lambda^s+2u^s\right)}{a^2}\left(2u_r+u_\theta\cot\theta+\frac{\partial u_\theta}{\partial\theta}\right)\Big|_{r=a}, \tag{23a}$$

$$\begin{aligned}\sigma_{r\theta}|_{r=a}=&\frac{1}{a^2}\left[\left(\lambda^s+\sigma^0\right)u_\theta+\left(\lambda^s+2\mu^s\right)\left(u_\theta\cot^2\theta-\frac{\partial^2u_\theta}{\partial\theta^2}-\cot\theta\frac{\partial u_\theta}{\partial\theta}\right)\right]\Big|_{r=a}\\&-\frac{1}{a^2}\left[\left(2\lambda^s+2\mu^s+\sigma^0\right)\frac{\partial u_r}{\partial\theta}\right]\Big|_{r=a},\end{aligned} \tag{23b}$$

for the simplified model SM-I and

$$\sigma_{rr}|_{r=a} = \frac{(2\lambda^s + 2u^s)}{a^2}\left(2u_r + u_\theta \cot\theta + \frac{\partial u_\theta}{\partial \theta}\right)\Big|_{r=a}, \tag{24a}$$

$$\sigma_{r\theta}|_{r=a} = \frac{1}{a^2}\left[\left(\lambda^s + \sigma^0\right)u_\theta + \left(\lambda^s + 2\mu^s - \sigma^0\right)\left(u_\theta \cot^2\theta - \frac{\partial^2 u_\theta}{\partial \theta^2} - \cot\theta \frac{\partial u_\theta}{\partial \theta}\right)\right]\Big|_{r=a}$$
$$-\frac{1}{a^2}\left[\left(2\lambda^s + 2\mu^s\right)\frac{\partial u_r}{\partial \theta}\right]\Big|_{r=a} \tag{24b}$$

for the simplified model SM-II.

Using the surface equilibrium condition, the coefficients A_n and B_n in Eq. (14) can be determined. In the far-field, the scattered waves can be asymptotically expressed as

$$\varphi^r = F_p(\theta, \varphi)\frac{e^{ik_p r}}{r} + o\left(\frac{1}{r}\right), \quad \chi^r = F_s(\theta, \varphi)\frac{e^{ik_s r}}{r} + o\left(\frac{1}{r}\right), \tag{25}$$

where

$$F_p(\theta, \varphi) = \sum_{n=0}^{\infty} \frac{1}{ik_p}(2n+1)A_n P_n(\cos\theta), \tag{26a}$$

$$F_s(\theta, \varphi) = \sum_{n=0}^{\infty} \frac{1}{ik_s}(2n+1)B_n P_n(\cos\theta) \tag{26b}$$

are the far-field amplitude of the scattered P and S waves, respectively.

4 The effective propagation constants in nanoporous materials

In the context of multiple scattering of waves, the total wave field at any point $\mathbf{r}$ in the matrix material can be expressed by

$$\mathbf{u}(\mathbf{r}; \mathbf{r}_1, \mathbf{r}_2, \ldots, \mathbf{r}_N) = \mathbf{u}^i(\mathbf{r}) + \sum_{k=1}^{N} \mathbf{T}^s(\mathbf{r}_k)\mathbf{u}^i(\mathbf{r}) + \sum_{m=1}^{N} \mathbf{T}^s(\mathbf{r}_m) \sum_{k=1, k\neq m}^{N} \mathbf{T}^s(\mathbf{r}_k)\mathbf{u}^i(\mathbf{r}) + \cdots, \tag{27}$$

where $\mathbf{T}^s(\mathbf{r}_k)$ is the scattering operator which transforms the incident wave into the scattered wave. The first term in Eq. (27) gives the incident wave, the second term gives the primary scattering wave of the incident wave, the third term is the rescattering wave of the incident wave and so on. The configurational average of the total wave field is

$$\langle \mathbf{u}(\mathbf{r}; \mathbf{r}_1, \ldots, \mathbf{r}_N)\rangle = \int \cdots \int \mathbf{u}(\mathbf{r}; \mathbf{r}_1, \ldots, \mathbf{r}_N) p(\mathbf{r}_1, \ldots, \mathbf{r}_N) \mathrm{d}V_1 \ldots \mathrm{d}V_N, \tag{28}$$

where $p(\mathbf{r}_1, \mathbf{r}_2, \ldots, \mathbf{r}_N)$ is the joint probability distribution of scatterers. The configurational average of the total wave field is called the averaged wave or coherent wave. In order to simplify the multiple scattering problems, the effective field approximation and the effective medium approximation are often used. Compared with the effective field approximation, the effective medium approximation results in two interfaces and thus makes the scattering problem of single scatterer more complicated. Therefore, the effective field approximation is used in this paper. In this approximation, each scatterer is assumed to be excited by an effective field. Then Eq. (27) can be approximately replaced by

$$\langle \mathbf{u}(\mathbf{r}; \mathbf{r}_1, \ldots, \mathbf{r}_N)\rangle = \mathbf{u}^i(\mathbf{r}) + \sum_{k=1}^{N} \mathbf{T}^s(\mathbf{r}_k)\mathbf{u}^e(\mathbf{r}|\mathbf{r}_k; \mathbf{r}_1, \cdots', \cdots, \mathbf{r}_N). \tag{29}$$

After performing the configurational average, we obtain the averaged wave

$$\langle \mathbf{u}(\mathbf{r}; \mathbf{r}_1, \ldots, \mathbf{r}_N)\rangle = \mathbf{u}^i(\mathbf{r}) + n \int \mathbf{T}^s(\mathbf{r}_k)\left\langle \mathbf{u}^e(\mathbf{r}|\mathbf{r}_k; \mathbf{r}_1, \cdots', \cdots, \mathbf{r}_N)\right\rangle \mathrm{d}V_k, \tag{30}$$

where n is the number density of scatterers and is related to the volume fraction f by $n = f/(4\pi a^3/3)$. The quantity $\left\langle \mathbf{u}^e(\mathbf{r}|\mathbf{r}_k; \mathbf{r}_1, \cdots' \cdots, \mathbf{r}_N)\right\rangle$ represents the exciting field acting on the kth scatterer averaged over all possible configurations of the other scatterers. Actually, it is the averaged total field with the absence of one scatterer and is not distinguished from the averaged total field when the number of scatterers is very large. Hence, Eq. (29) becomes a self-consistent equation. The wave number of the coherent wave can be estimated by means of an iterative process [1]

$$\left(\frac{k_p^{(i+1)}}{k_p^{(i)}}\right)^2 = \left(1 + \frac{2\pi n}{(k_p^{(i)})^2} F_p^{(i)}(0,\phi)\right)^2 - \left(\frac{2\pi n}{(k_p^{(i)})^2} F_p^{(i)}(\pi,\phi)\right)^2, \tag{31}$$

where $F_p^{(i)}(0,\varphi)$ and $F_p^{(i)}(\pi,\varphi)$ are the forward and backward scattering amplitudes of the individual scatterer. To start the iteration, the initial value $k_p^{(0)}$ is taken to be that in the matrix material. The effective wave number k_p^* can be obtained by repeating the iterative process until the convergence condition, namely, $\left|(k_p^{(i+1)} - k_p^{(i)})/k_p^{(i)}\right| < \delta$, is satisfied.

The effective wave numbers are associated with the expansion coefficient of the scattered waves and are complex value, in general. The imaginary part of the complex wavenumber means that the averaged wave is a decaying wave. In other word, the energy carried by the averaged wave decreases gradually when it propagates in a randomly distributed nanoporous material just like that the viscoelastic wave propagates in a viscoelastic medium. However, it should be noted that the attenuation of viscoelastic wave results from the dissipation of material but the attenuation of the averaged wave results from the multiple scattering effects of the randomly distributed nanocavities. The phase speed and the attenuation of the averaged wave are our main concern. The normalized effective speed and attenuation of the averaged P waves can be expressed as

$$c_p^*/c_p = \mathrm{Re}\left(k_p/k_p^*\right), \quad \alpha_p = \mathrm{Im}\left(k_p^*/k_p\right). \tag{32}$$

The effective dynamic modulus of nanoporous composites can be obtained by

$$\frac{K^*}{K} = \frac{\rho^*}{\rho}\left\{\left(\mathrm{Re}\left(\frac{k_p}{k_p^*}\right)\right)^2 + \frac{4}{3}\frac{\mu}{K}\left[\left(\mathrm{Re}\left(\frac{k_p}{k_p^*}\right)\right)^2 - \left(\mathrm{Re}\left(\frac{k_s}{k_s^*}\right)\right)^2\right]\right\}, \tag{33}$$

where the effective density $\rho^* = (1-f)\rho$. μ and K are the shear modulus and the bulk modulus of the matrix material, respectively. K^* is the effective dynamic elastic modulus of the nanoporous composites. It should be pointed out that the effective dynamic modulus should tend to the effective static modulus when the normalized wavenumber ka tends to zero. The effective static modulus of the nanocomposites with the interface energy effects considered can be estimated by the Mori-Tanaka method, namely [25],

$$\bar{K} = K_0 + f(\bar{K}_1 - K_0)A_m, \tag{34}$$

where $\bar{K}_1 = K_1 + 2(\sigma^0 + 2\lambda^s + 2\mu^s)/3a$ is the equivalent bulk modulus of the inclusion when the interface energy effects is taken into consideration and K_1 is the bulk modulus of the inclusion without consideration of the interface energy effects. In the present study, K_1 is taken to be zero for cavities. K_0 is the bulk modulus of the matrix material. The strain concentration factor can be written as

$$A_m = \frac{K_0}{K_0 + (1+f)(\bar{K}_1 - K_0)S_m}, \quad S_m = \frac{3K_0}{3K_0 + 4\mu_0}. \tag{35}$$

5 Results and discussion

In this numerical example, the matrix material is assumed to be isotropic aluminum ($\rho = 2706\mathrm{kg/m}^3$, $\mu = 26.7\mathrm{GPa}$, $\lambda + 2\mu = 110.5\mathrm{GPa}$). The iterative stop condition of Eq. (31) is $\left|(k_p^{(i+1)} - k_p^{(i)})/k_p^{(i)}\right| < 0.001$. Three parameters, namely $k_1 = \frac{\lambda^s + 2\mu^s}{2\mu a}$, $k_2 = \frac{\lambda^s}{2\mu a}$ and $k_3 = \frac{\sigma^0}{2\mu a}$, are introduced to characterize the properties of the surface. Atomic simulations demonstrated that the elastic constants λ^s and μ^s can be either positive or negative, λ^s/μ and μ^s/μ are in the order of angstroms (10^{-10}m) [27]. For a macroscopic cavity, the parameter

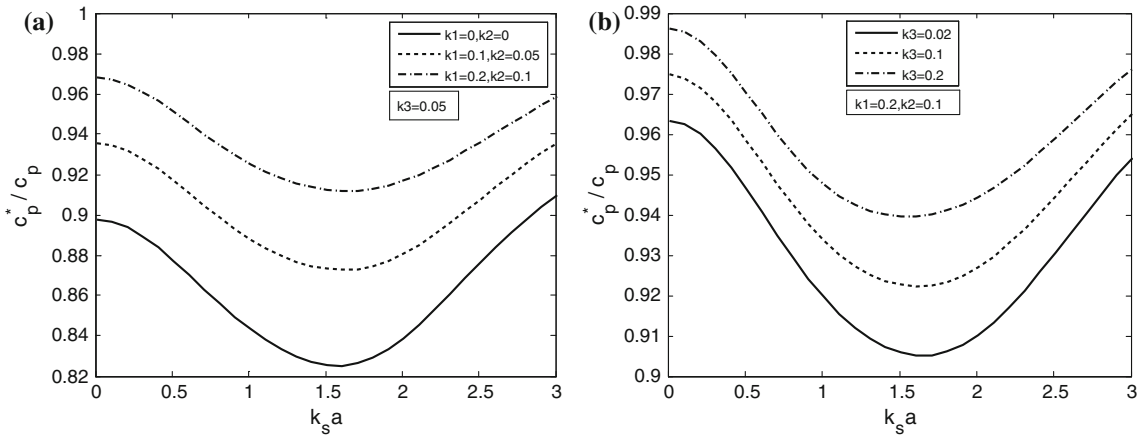

Fig. 1 Effective speed of coherent P wave obtained for different surface characteristic parameters (the porosity $f = 0.3$). **a** Effects of surface elastic constants (λ^s and μ^s). **b** Effects of surface residual stress (σ^0)

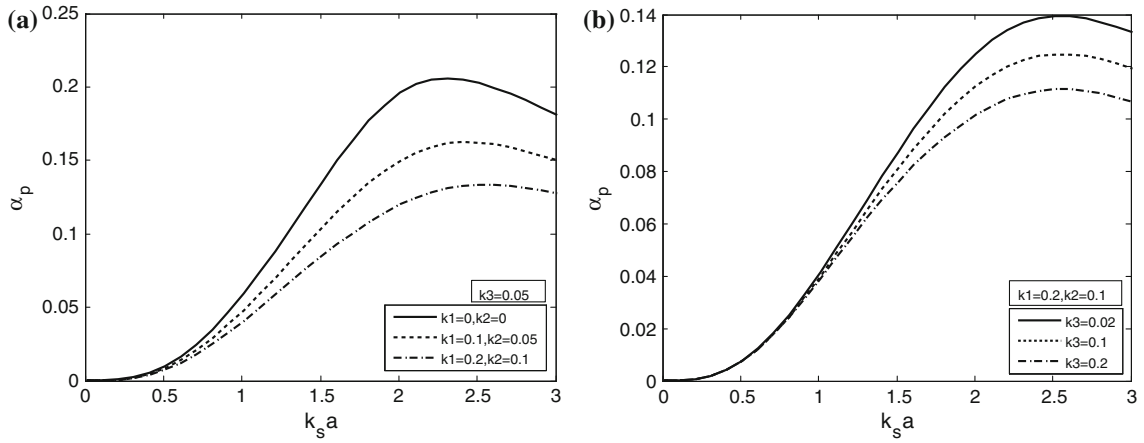

Fig. 2 Effective attenuation of coherent P wave obtained for different surface characteristic parameters (the porosity $f = 0.3$). **a** Effects of surface elastic constants (λ^s and μ^s). **b** Effects of surface residual stress (σ^0)

k_1 and k_2 tend to zero because $(\lambda^s + 2\mu^s)/\mu$ and λ^s/μ are very small. The surface effects disappear and Eq. (22) reduces to the solution of the classical elasticity theory without the surface effects. However, the parameter k_1 and k_2 increase gradually and become notable when the radius of cavity, a, shrinks to nanometers. In this situation, the surface effect becomes significant and can not be ignored anymore.

Figure 1 shows that the propagation speed of the coherent P wave increases due to the surface effect in the frequency range considered. It is also noticed that the propagation speed is influenced not only by the surface elastic constants λ^s and μ^s, which represent the surface elasticity, but also by the residual surface tension σ^0. The surface effects on the attenuation of coherent P wave are shown in Fig. 2. It is noted that the attenuation coefficient has a peak value within the frequency range considered. Both the surface elasticity reflected by the surface elastic constants (λ^s, μ^s) and the residual surface tensor σ^0 make the peak of attenuation decreasing. If the inhomogenous material with randomly positioned spherical cavities is replaced by a homogenous solid medium, and keep the same propagation constants (speed and attenuation), the equivalent homogenous solid medium should have complex elastic constants just like a viscoelastic material. The real part of the elastic constant represents the actual elastic modulus, and the imaginary part of the elastic constant represents the attenuation nature of the equivalent homogeneous solid medium.

Figures 3 and 4 are the effective speed and effective attenuation obtained from the simplified model SM-I. Compared with Figs. 1 and 2, it is found that the effective speed obtained from the simplified model SM-I is smaller than that from the Huang's model and the effective attenuation obtained from SM-I is greater than that from Huang's model for the same surface parameters, although these differences between the two models are very small for relative smaller surface residual stress σ^0 but increase gradually as the surface residual stress

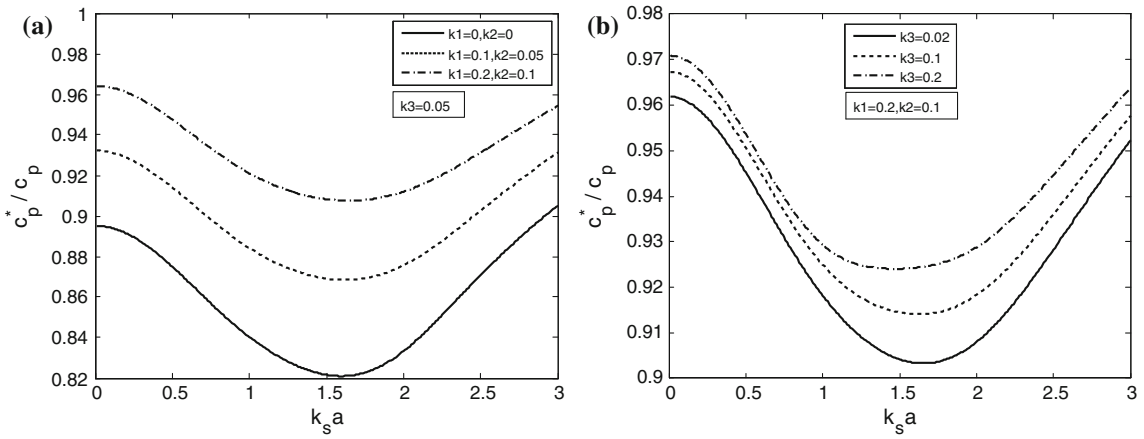

Fig. 3 Effective velocity of coherent P wave obtained from the simplified model SM-I for different surface characteristic parameters (the porosity $f = 0.3$). **a** Effects of surface elastic constants (λ^s and μ^s). **b** Effects of surface residual stress (σ^0)

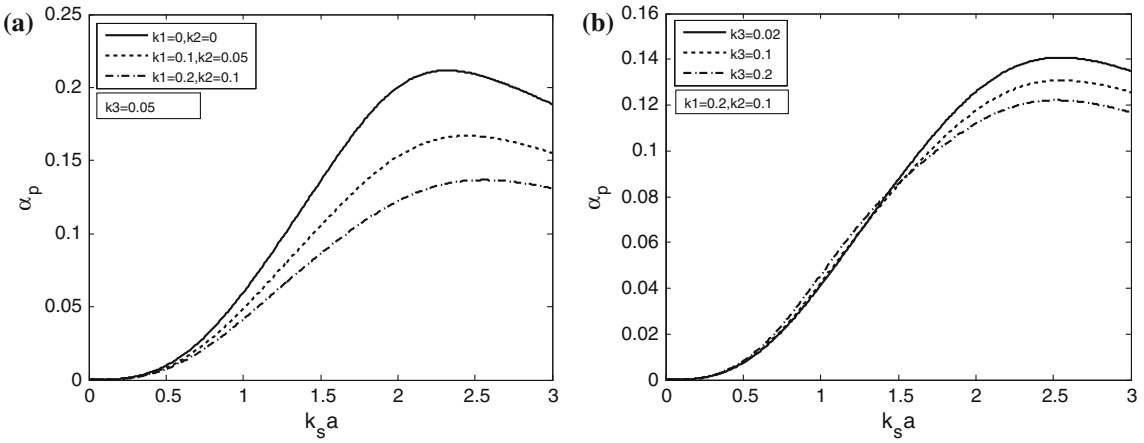

Fig. 4 Effective attenuation of coherent P wave obtained from the simplified model SM-I for different surface characteristic parameters (the porosity $f = 0.3$). **a** Effects of surface elastic constants (λ^s and μ^s). **b** Effects of surface residual stress (σ^0)

σ^0 increases. The observation implies that the effects of out-of-plane parts of the surface stress on the effective speed and attenuation are not prominent under relative smaller surface residual stress σ^0.

Figures 5 and 6 are the effective speed and effective attenuation obtained from the simplified model SM-II. Compared with Figs. 3 and 4, it is found that the effective speed decreases and the effective attenuation increases and the differences become more pronounced as the surface residual stress σ^0 increases. The observation implies that the non-symmetrical term in the in-plane surface stress, i.e., $\sigma^0(\mathbf{u}\nabla_{0s})^{(\mathrm{in})}$ in Eq. (5), has evident influences on the effective speed and attenuation. Compared with the out-of plane term, i.e., $\sigma^0(\mathbf{u}\nabla_{0s})^{(\mathrm{out})}$, the non-symmetrical term in the in-plane surface stress plays a more important role.

Figure 7 shows the dynamic effective bulk modulus of the porous material for different surface elastic constants and the residual surface stresses. Similar to the discussion on the effective speed, both the surface elastic constants (λ^s and μ^s) and the surface residual stress (σ^0) influence the bulk modulus, and in general, the bulk modulus increases with the increasing of these parameters. This implies that the porous material becomes harder and thus the coherent wave propagates faster when the surface effect are considered if the surface elastic constants (λ^s and μ^s) and the surface residual stress (σ^0) are assumed to be positive.

In order to study the size effect of nanocavity on the effective dynamic bulk modulus of the porous composites, the relationship between the normalized effective dynamic elastic modulus K^*/K (K is the bulk modulus of the matrix material) and the radius of spherical cavity at a fixed volume fraction ($f = 0.3$) is shown in Fig. 8. In the numerical calculation, the surface parameters are taken to be $\lambda^s = 6.84$ (N/m), $\mu^s = -0.376$ (N/m) and $\sigma^0 = 0.05$ (J/m^2) [28]. In order to compare with the static effective bulk modulus, the static effective bulk modulus [obtained from Eq. (34)] is also calculated and shown in Fig. 8. K^*_{dynamic} and K^*_{static} are

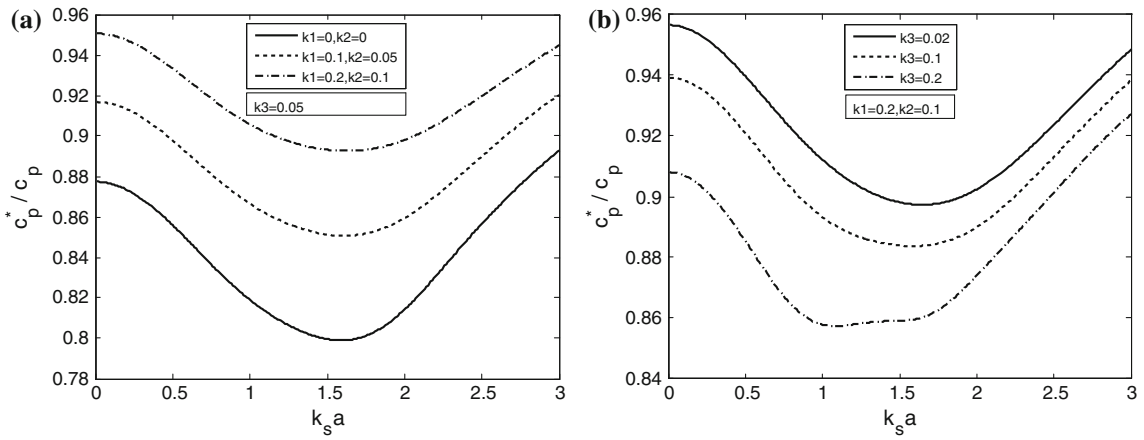

Fig. 5 Effective velocity of coherent P wave obtained from the simplified model SM-II for different surface characteristic parameter (the porosity $f = 0.3$). **a** Effects of surface elastic constants (λ^s and μ^s). **b** Effects of surface residual stress (σ^0)

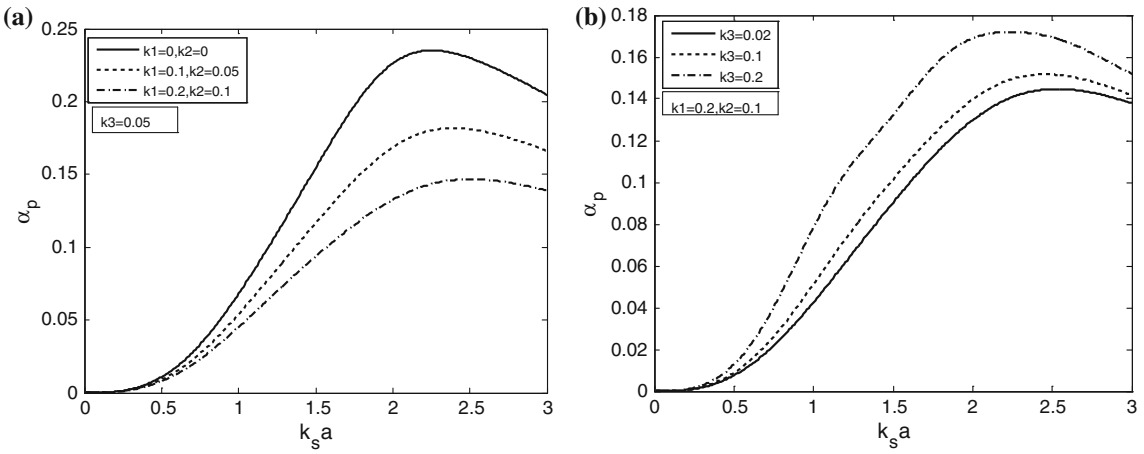

Fig. 6 Effective attenuation of coherent P wave obtained from the simplified model SM-II for different surface characteristic parameter (the porosity $f = 0.3$). **a** Effects of surface elastic constants (λ^s and μ^s). **b** Effects of surface residual stress (σ^0)

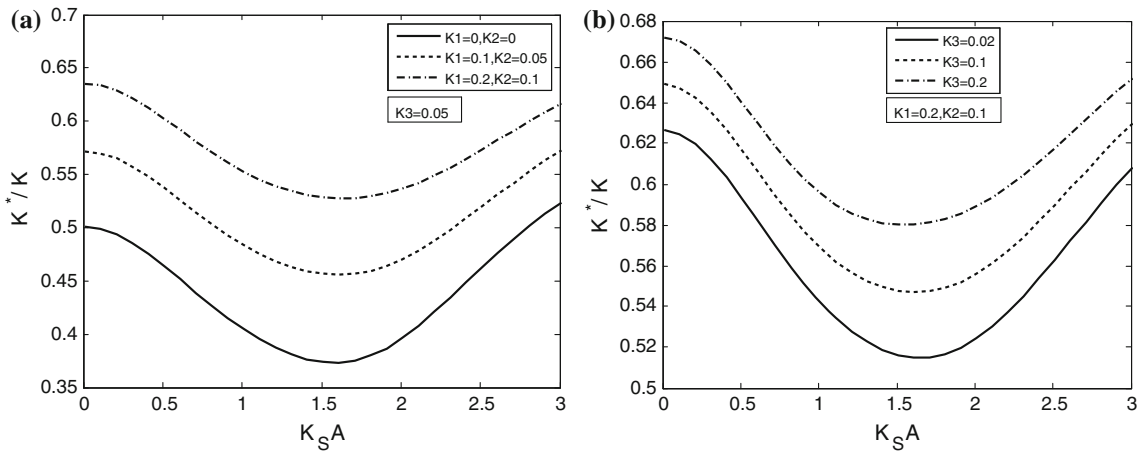

Fig. 7 Dynamic effective bulk modulus of nanoporous material obtained for different surface characteristic parameters (the porosity $f = 0.3$). **a** Effects of surface elastic constants (λ^s and μ^s). **b** Effects of surface residual stress (σ^0)

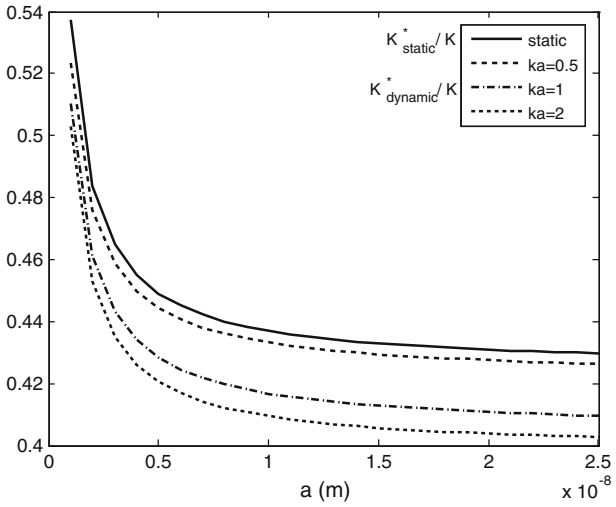

Fig. 8 Comparison between the normalized static effective modulus and the normalized dynamic effective modulus (the porosity $f = 0.3$)

the effective dynamical bulk modulus and the effective static bulk modulus with the surface effects considered, respectively. It is observed that the surface effect is prominent when the radius of the nanocavities decreases to nanoscale. It is also noted that the surface effect is more evident for the effective dynamic modulus than for the effective static modulus. As it is expected, the effective dynamic bulk modulus reduces to the corresponding effective static bulk modulus at a long wave limit $k_s a \to 0$. This can be seen as a validation of our numerical results to some extent.

6 Conclusions

The surface effects on the effective propagation constants of the coherent P wave in a nanoporous material with randomly positioned spherical cavities are studied. The surface effects include the effects of the surface elasticity and the effects of residual surface tension. The previous works about the surface effects on the wave motion problem only concerned with the surface elasticity and the residual surface tension were rarely considered. In this paper, both surface elasticity and the residual surface tension are discussed. The numerical results show that both the surface elasticity and the residual surface tension influence evidently the effective propagation constants of the coherent waves. In general, the surface elasticity and the residual surface tension make the propagation speed increasing and the attenuation coefficient decreasing. The surface stresses are non-symmetrical and include an in-plane part and an out-of-plane part. The non-symmetrical part of the in-plane surface stress is important and cannot be ignored, in general. The out-of-plane part of the surface stress is less important compared with the non-symmetrical part and can be ignored at relative smaller surface residual stress. However, both should be considered when the surface residual stress is relative larger. Moreover, the bulk modulus of the equivalent homogenous solid medium with same propagation speed and attenuation of the porous material becomes larger when the surface stress and the residual surface tension are considered. By comparison with the static effective bulk modulus, it is observed that both the static effective modulus and the dynamic effective modulus increase evidently when the size of the cavities shrinks to nanoscale. However, the size effects are more pronounced for the effective dynamic bulk modulus than for the effective static bulk modulus.

Acknowledgments The authors are highly thankful to professor Huang about the discussion of many details on the surface stress model. The project was supported by the National Natural Science Foundation of China (10972029) and Opening fund of State Key Laboratory of Nonlinear Mechanics (LNM).

References

1. Waterman, P.C., Truell, R.: Multiple scattering of waves. J. Math. Phys. **2**(4), 512–537 (1961)

2. Datta, S.K., Ledbetter, H.M., Shindo, Y.: Phase velocity and attenuation of elastic waves in a particle-reinforced composite medium. Wave Motion **10**(2), 171–182 (1988)
3. Shindo, Y., Nozaki, H., Datta, S.K.: Effect of interface layers on elastic wave propagation in a metal matrix composite reinforced by particles. J. Appl. Mech. **62**(1), 178–185 (1995)
4. Sato, H., Shindo, Y.: Multiple scattering of elastic waves in a particle-reinforced composite medium with graded interfacial layers. Mech. Mater. **35**, 82–106 (2003)
5. Wei, P.J., Huang, Z.P.: Dynamic modulus of the particle-reinforced composites with the viscoelastic interphase. Int. J. Solids Struct. **41**(24–25), 6993–7007 (2004)
6. Varadan, V.K., Ma, Y., Varadan, V.V.: A multiple scattering theory for elastic waves propagation in discrete random medium. J. Acoust. Soc. Am. **77**, 375–385 (1985)
7. Kanaun, S.K.: Dielectric properties of matrix composite materials with high volume concentrations of inclusions (effective field approach). Int. J. Eng. Sci. **41**, 1287–1312 (2003)
8. Fang, X.Q., Wang, D.B., Liu, J.X.: Multiple scattering of elastic waves in metal-matrix composite materials with high volume concentration of particles. Eur. J. Mech. A Solids **28**, 377–386 (2009)
9. Shuttleworth, R.: The surface tension of solids. Proc. Phys. Soc. A **63**, 444–457 (1950)
10. Gurtin, M.E., Murdoch, A.I.: A continuum theory of elastic material surfaces. Arch. Rat. Mech. Anal. **57**, 291–323 (1975)
11. Gurtin, M.E., Murdoch, A.I.: Surface stress in solids. Int. J. Solids Struct. **14**, 431–440 (1978)
12. Cahn, J.W., Larche, F.: Surface stress and the chemical equilibrium of small crystals. Acta Metall. **30**, 51–56 (1982)
13. Nix, W.D., Gao, H.J.: An atomistic interpretation of interface stress. Scr. Mater. **39**, 1653–1661 (1998)
14. Cammarata, R.C., Sieradzki, K., Spaepen, F.: Simple model for interface stress. J. Appl. Phys. **87**, 1227–1234 (2000)
15. Duan, H.L., Wang, J., Huang, Z.P., Karihaloo, B.L.: Size-dependent effective elastic constants of solids containing nano-inhomogeneities with interface stress. J. Mech. Phys. Solids **53**, 1574–1596 (2005)
16. Huang, Z.P, Sun, L.: Size-dependent effective properties of a heterogeneous material with interface energy effect: from finite deformation theory to infinitesimal strain analysis. Acta Mech. **190**, 151–163 (2007)
17. Gao, X., Hao, F., Fang, D.N., Huang, Z.P.: Boussinesq problem with the surface effect and its application to contact mechanics at the nanoscal. Int. J. Solids Struct. **50**, 2620–2630 (2013)
18. Ru, C.Q.: Simple geometrical explanation of Gurtin-Murdoch model of surface elasticity with clarification of its related versions. Sci. China Phys. Mech. Astron. **53**, 536–544 (2010)
19. Wang, G.F.: Diffraction of plane compressional wave by a nanosized spherical cavity with surface effects. Appl. Phys. Lett. **90**, 211907 (2007)
20. Wang, G.F.: Diffraction of shear waves by a nanosized spherical cavity. Appl. Phys. Lett. **103**, 053519 (2008)
21. Qiang, F.W., Wei, P.J., Li, L.: The effective propagation constants of SH wave in composites reinforced by dispersive parallel nanofibers. Sci. China Phys. Mech. Astron. **55**(7), 1172–1177 (2012)
22. Qiang, F.W., Wei, P.J.: Propagation of elastic wave in nanoporous material with distributed cylindrical nanoholes. Sci. China Phys. Mech. Astron. **56**, 1542–1550 (2013)
23. Hasheminejad, S.M., Avazmohammadi, R.: Size-dependent effective dynamic properties of unidirectional nanocomposites with interface energy effects. Compos. Sci. Tech. **69**, 2538–2546 (2009)
24. Huang, Z.P., Wang, J.: A theory of hyperelasticity of multi-phase media with surface/interface energy effects. Acta Mech. **182**, 195–210 (2006)
25. Huang, Z.P., Wang, J.: Micromechanics of nanocomposites with interface energy effect. In: Li, S.F., Gao, X.L. (eds.) Handbook of Micromechanics and Nanomechanics, pp. 303–348. Pan Stanford Publishing Pte Ltd., Singapore (2013)
26. Hoger, A.: On the determination of residual stress in an elastic body. J. Elast. **16**, 303–324 (1986)
27. Shenoy, V.B.: Atomistic calculations of elastic properties of metallic fcc crystal surfaces. Phys. Rev. B **71**(094104), 1–14 (2005)
28. Cai, B., Wei, P.J.: Surface/interface effects on dispersion relations of 2D phononic crystal with parallel nanofibers. Acta Mech. **224**(11), 2749–2758 (2013)